



# Numerical investigation of Heat transfer effect on MHD flow of two types of visco-elastic fluid over a stretching sheet through porous media

<sup>1</sup>B. Mohanty, <sup>2</sup>S.R.Mishra and <sup>3</sup>H.B. Pattnaik

<sup>1</sup>Research Scholar, P.G. Department of Mathematics, Ravenshaw University, Cuttack, Orissa, India

<sup>2</sup>Department of Mathematics, I.T.E.R, Siksha 'O' Anusandhan University, Khandagiri, Bhubaneswar, Orissa, India

<sup>3</sup>Department of Mathematics, KIIT University, Bhubaneswar, India

E-mail: satyaranjan\_mshr@yahoo.co.in

**Abstract** -An investigation has been made to study the heat transfer effect in a boundary layer flow through porous medium of an electrically conducting visco-elastic fluid subject to transverse magnetic field in the presence of heat source. We have studied the effects of radiation, viscous and Joule dissipation and internal heat generation / absorption. Closed form solutions for the boundary layer equations of the flow are presented for two classes of visco-elastic fluid, namely, the second-grade and Walters  $B'$  fluid. The method of solution involves similarity transformation. The coupled non-linear partial differential equations representing momentum and concentration and non homogeneous heat equation are reduced into set of non-linear ordinary differential equations. The transformed equations are solved numerically by using Runge-Kutta sixth order with shooting technique. The comparison has been made with the confluent hypergeometric (Kummer's) function. The exact solution of temperature field are obtained for prescribed surface temperature (PST) as well as prescribed surface heat flux (PHF) boundary condition. The interaction of magnetic field is proved to be counter productive in enhancing velocity distribution, whereas presence of porous matrix reduces the temperature field at all points.

**Key words:** Heat source, Porous medium, Second grade / Walters  $B'$  Visco-elastic, Kummer's function.

## I. INTRODUCTION

The fluid flow over a stretching sheet is important in many practical applications such as extrusion of plastic sheets, paper production, glass blowing, metal spinning, polymers in metal spring processes, the continuous casting of metals, drawing plastic films and spinning of fibers (Paulet and Weidman, [1]). The quality of the final product depends on the rate of heat transfer at the stretching surface. The problem of stretching surface with constant surface temperature was analyzed by Crane [2]. The growing need for chemical reaction and hydrometallurgical industries requires the study of heat and mass transfer with chemical reaction. There are many transport processes that are governed by the combined action of buoyancy forces due to both thermal and mass diffusion in the presence of chemical reaction effect. These processes are observed in the nuclear reactor safety and combustion systems, solar collectors, as well as metallurgical and chemical engineering.

### Nomenclature

$K'_p$	permeability of the medium	$K_p$	porosity parameter
$K$	thermal diffusivity	$Mn$	magnetic parameter
$R_c$	elastic parameter	$B_0$	magnetic field strength
$P_r$	Prandtl number	$Q$	heat source/sink parameter
$S_c$	Schmidt number	$T'$	temperature of the field
$T$	non-dimensional temperature	$t'$	time
$t$	non-dimensional time	$k_0$	dimensionless elastic parameter
$\rho$	density of the fluid	$q_r$	radiative heat flux
$\nu$	kinematics coefficient of viscosity	$k_1$	absorption coefficient
$\sigma^*$	Stefan-Boltzmann constant	$\sigma$	electrical conductivity
$C_p$	specific heat	$R$	radiation parameter

$q_w$	wall heat flux	$E_c$	Eckert number
$\tau_w$	wall shear stress	$C_f$	skin friction coefficient
$T_\infty$	temperature far from sheet	$T_w$	wall temperature
$q$	dimensional heat source/sink parameter	$u_w$	velocity of the sheet

Ishak et al [3] investigated theoretically the unsteady mixed convection boundary layer flow and heat transfer due to a stretching vertical surface in a quiescent viscous and incompressible fluid. Mahapatra and Gupta ([4], [5]) considered the stagnation flow on a stretching sheet. Sammer [6] investigated the heat and mass transfer over an accelerating surface with heat source in presence of magnetic field. Wang [7] studied the stagnation flow towards a shrinking sheet.

Naseem and Khan [8] investigated boundary layer flow past a stretching plate with suction, heat and mass transfer and with variable conductivity. Elbashbeshy and Bazid [9] studied flow and heat transfer in a porous medium over a stretching surface with internal heat generation and suction/blowing. Cortell [10] also reported the flow and heat transfer of a fluid through porous medium over a stretching surface with internal heat generation. Anjali Devi and Ganga [11] have studied the viscous dissipation effect on nonlinear MHD flow in a porous medium over a stretching porous surface.

Mushtaq et al. [12] examined the effects of thermal buoyancy on visco-elastic flow of a second grade fluid past a vertical, continuously stretching sheet. Numerical solutions for the coupled nonlinear partial differential are generated by using local non-similarity method and Keller-Box scheme. Hayat et al. [13] applied an analytic technique, namely homotopy analysis method (HAM), to study the steady mixed convection in two dimensional stagnation flows of a second grade fluid around a heated surface with the wall temperature varying linearly with the distance from the stagnation point. An investigation has been conducted by Arnold et al. [14] on the visco-elastic fluid flow and heat transfer characteristics over a stretching sheet taking into account the effects of frictional heating and internal heat generation/absorption. Battaler [15] investigated the effect of thermal radiation on heat transfer in a boundary layer visco-elastic second order fluid over a stretching sheet with internal heat source/sink. Recently, we explore the flow of a Jeffery fluid [16-17] over a stretched sheet subject to power law temperature in the presence of heat source/sink.

The present study considers the flow of a visco-elastic incompressible electrically conducting fluid flow past a stretching sheet through a porous medium in the presence of magnetic field, viscous dissipation, uniform

heat source/sink, surface fluid suction/injection. The aim of the following discussion is to bring out the effect of permeability of the medium and plate temperature on the flow phenomena.

## II. FORMULATION OF THE PROBLEM

Let us consider for an incompressible visco-elastic fluid given by Coleman and Noll [18]:

$$T = -pI + \mu A_1 + \alpha_1 A_2 + \alpha_2 A_1^2, \quad (1)$$

where  $T$ , the Cauchy tensor,  $p$ , the pressure  $\mu$ , the viscosity,  $\alpha_1$  and  $\alpha_2$  are two normal stress moduli with  $\alpha_1 < 0$  and  $A_1$  and  $A_2$  are first two Rivlin-Ericksen tensors [19] defined by

$$\left. \begin{aligned} A_1 &= \nabla v + (\nabla v)^T \\ A_2 &= \frac{dA_1}{dt} + A_1 \cdot \nabla v + (\nabla v)^T \cdot A_1 \end{aligned} \right\} \quad (2)$$

Here  $v$  is the velocity,  $\nabla$  the gradient operator and  $(d/dt)$  the material time derivative. Dunn and Fosdick [20] found that the material moduli satisfy the following condition

$$\mu \geq 0, \alpha_1 \geq 0, \alpha_1 + \alpha_2 = 0. \quad (3)$$

But for many of the non-Newtonian fluids of Rheological interest, the experimental results for  $\alpha_1$  and  $\alpha_2$  donot satisfy the restrictions (3). In case of second order fluid the material moduli should satisfy

$$\mu \geq 0, \alpha_1 \leq 0, \alpha_1 + \alpha_2 \neq 0. \quad (4)$$

Generally, in the literature the fluid satisfied the model equation (1) with  $\alpha_1 < 0$  is termed as second-order and  $\alpha_1 > 0$  is termed as second-grade fluid. When  $\alpha_1 = 0$ ,  $\alpha_2 = 0$  and  $\mu > 0$ , equation (1) reduces to the well-known constitutive relation of an incompressible Newtonian fluid. Another class of model is the rate-type fluid models, such as Walters B', which presents an approximation to the first order in elasticity, i.e. for short or rapidly fading memory fluids. The steady two-dimensional boundary layer equations for Walters B' were derived by Beard and Walters [21].

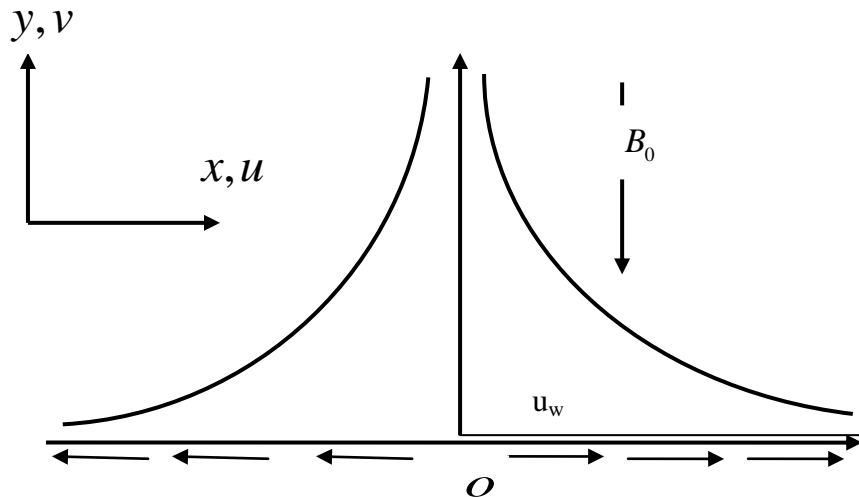


Fig.1 Physical model and co-ordinate system

Consider the steady two-dimensional boundary layer flow of an electrically conducting, visco-elastic fluid past over a stretching sheet through porous medium coinciding with the plane, the flow being confined to two equal and opposite forces are applied along  $x$ -axis so that the surface is stretched, keeping the origin fixed. A uniform magnetic field strength  $B_0$  is imposed along  $y$ -axis, which produces magnetic effect in the

$x$ -direction. Under the usual boundary layer assumptions, the conservation equations of mass, momentum and energy for the flow of visco-elastic fluid, in the usual notation, can be written as

$$\frac{\partial u}{\partial x} + \frac{\partial v}{\partial y} = 0, \quad (5)$$

$$u \frac{\partial u}{\partial x} + v \frac{\partial u}{\partial y} = \nu \frac{\partial^2 u}{\partial y^2} - \frac{\sigma B_0^2 u}{\rho} - \frac{\nu}{K_p} u + \frac{k_0}{\rho} \left( \frac{\partial}{\partial x} \left( u \frac{\partial^2 u}{\partial y^2} \right) + v \frac{\partial^3 u}{\partial y^3} + \frac{\partial u}{\partial y} \frac{\partial^2 u}{\partial x \partial y} \right), \quad (6)$$

$$\begin{aligned} \rho C_p \left( u \frac{\partial T}{\partial x} + v \frac{\partial T}{\partial y} \right) = & K \frac{\partial^2 T}{\partial y^2} + \mu \left( \frac{\partial u}{\partial y} \right)^2 + k_0 \left( \frac{\partial u}{\partial y} \frac{\partial}{\partial y} \left( u \frac{\partial u}{\partial x} + v \frac{\partial u}{\partial y} \right) \right) \\ & + \sigma B_0^2 u^2 - \frac{\partial q_r}{\partial y} + q(T - T_\infty), \end{aligned} \quad (7)$$

Rosseland's approximation for thermal radiation [15] gives  $q_r = -\frac{4\sigma^*}{3k_1} \frac{\partial T^4}{\partial y}$ . It is assumed that the temperature variation within the flow of is such that  $T^4$  may be expanded in a Taylor's series. Expanding  $T^4$  about  $T_\infty$  and neglecting the higher order terms, we have  $T^4 = 4T_\infty^3 T - 3T_\infty^4$  and  $\frac{\partial q_r}{\partial y} = \frac{16\sigma^* T_\infty^3}{3k_1 \rho C_p} \frac{\partial^2 T}{\partial y^2}$ .

Therefore equation (7) reduces to

$$\begin{aligned} u \frac{\partial T}{\partial x} + v \frac{\partial T}{\partial y} = & \alpha \frac{\partial^2 T}{\partial y^2} + \frac{\mu}{\rho C_p} \left( \frac{\partial u}{\partial y} \right)^2 + \frac{k_0}{\rho C_p} \left( \frac{\partial u}{\partial y} \frac{\partial}{\partial y} \left( u \frac{\partial u}{\partial x} + v \frac{\partial u}{\partial y} \right) \right) \\ & + \frac{16\sigma^* T_\infty^3}{3k_1 \rho C_p} \frac{\partial^2 T}{\partial y^2} + \frac{q}{\rho C_p} (T - T_\infty) + \frac{\sigma B_0^2}{\rho C_p} u^2 \end{aligned} \quad (8)$$

where  $k_1$  is the mean absorption coefficient and the boundary conditions are

$$\left. \begin{aligned} u = u_w = Ex, v = v_w, T = T_w(x) \quad & \text{at } y = 0 \\ u = 0, \frac{\partial u}{\partial y} = 0, T \rightarrow T_\infty, \quad & \text{as } y \rightarrow \infty \end{aligned} \right\} \quad (9)$$

where  $E$ , the positive constant,  $v_w$ , the suction velocity.

### III. SOLUTION OF THE FLOW FIELD

Equations (5) and (6) admit self-similar solutions of the form  $f = \frac{\psi}{\nu \sqrt{\text{Re}_x}}, \eta = \frac{y}{x} \sqrt{\text{Re}_x}$  (10)

where  $f$  is the dimensionless stream function and  $\eta$  is the similarity variable and  $\text{Re}_x = u_w x / \nu$  is the local Reynolds number. Substituting in (6), we get

$$f''' + ff'' - f'^2 + R_c \{2ff''' - f''^2 - ff^{iv}\} - \left(Mn + \frac{1}{K_p}\right) f' = 0, \quad (11)$$

where  $R_c = k_0 E / \mu$ , the visco-elastic parameter,  $Mn = \sigma B_0^2 / \rho E$ , the magnetic parameter and  $K_p = K_p^* / \rho E$ , the permeability parameter. The corresponding boundary conditions are:

$$f(0) = f_w, f'(0) = 1, f'(\infty) = 0, f''(\infty) = 0. \quad (12)$$

where  $f_w = -\nu \sqrt{\text{Re}_x} / u_w$  is the suction / injection parameter. A positive value of represents suction and negative value stands for injection. The exact solution (9) with boundary conditions (10) is obtained following Chakrabati and Gupta [22] in the form  $f(\eta) = \frac{1 - e^{-r\eta}}{r} + f_w$ ,

$$f(\eta) = \frac{1 - e^{-r\eta}}{r} + f_w, \quad (13)$$

where  $r$  is a real positive root of the cubic algebraic equation:

$$R_c f_w r^3 + (R_c + 1)r^2 - f_w r - (1 + Mn + 1/K_p) = 0. \quad (14)$$

### IV. SKIN FRICTION

The shear stress at the wall is defined as

$$\tau_w = \mu \left( \frac{\partial u}{\partial y} \right)_{y=0} = \mu \alpha \sqrt{a/\nu} f''(0) \quad (15)$$

The non dimensional form of skin friction,  $C_f$  at the wall is  $C_f = \tau_w / \mu \alpha \sqrt{a/\nu} = f''(0) = -r$ .

### V. HEAT TRANSFER ANALYSIS

Case I: Power-law Surface Temperature (PST)

In power-law surface temperature introducing non-dimensional quantities  $\theta(\eta) = \frac{T - T_\infty}{T_w - T_\infty}$ ,  $P_r = \mu C_p / K$ ,

$Q = \frac{\mu \nu^2}{\nu(T_w - T_\infty)}$ ,  $E_c = \frac{E^2 L^2}{AC_p}$ ,  $R = \frac{16\sigma_1 T_\infty^3}{3\alpha_R k}$  and using equation (10) the equation (8) becomes

$$(1 + R)\theta'' + P_r f \theta' + P_r (Q - 2f')\theta = -E_c P_r (f''^2 + R_c(ff'' - ff''') + (Mn + 1/K_p)f'^2) \quad (16)$$

The boundary conditions are  $\theta(0) = 1, \theta(\infty) = 0$ . (17)

Introducing the variable  $\xi = -\frac{P_r e^{-\alpha\eta}}{(1 + R)r^2}$ , equation (16) transformed to

$$\begin{aligned} \xi \frac{d^2 \theta}{d\xi^2} + \left(1 - \frac{P_r}{(1 + R)r^2} - \xi\right) \frac{d\theta}{d\xi} + \left(\frac{P_r Q}{(1 + R)r^2 \xi} + 2\right) \theta \\ = -\frac{E_c (1 + R)r^2}{P_r} (1 + R_c S + Mn + 1/K_p) \xi \end{aligned} \quad (18)$$

with the boundary conditions

$$\theta\left(\xi = -\frac{P_r}{(1 + R)r^2}\right) = 1, \theta(\xi = 0) = 0 \quad (19)$$

Using confluent hypergeometric function we get,

$$\theta(\xi) = \left[ 1 + \frac{E_c P(1 + R_c S + \left( Mn + \frac{1}{K_p} \right) / r^2)}{(1 + R)(4 - (2S - Q)P_r^*)} \right] \left( \frac{\xi}{-P_r^*} \right)^a \frac{M(a - 2, 1 + b, \xi)}{M(a - 2, 1 + b, -P_r^*)} \quad (20)$$

$$- \frac{E_c P(1 + R_c S + \left( Mn + \frac{1}{K_p} \right) / r^2)}{(1 + R)(4 - (2S - Q)P_r^*)} \left( \frac{\xi}{P_r^*} \right)^2$$

$$\text{where, } a = \frac{P_r^* S + \sqrt{(P_r^* S)^2 - 4P_r^* Q}}{2}, b = \sqrt{(P_r^* S)^2 - 4P_r^* Q}, P_r^* = \frac{P_r}{(1 + R)r^2}, S = 1 + rf_w$$

and  $M(\alpha_1, \alpha_2; x)$  denotes the Kummer's Function

$$M(\alpha_1, \alpha_2; x) = \sum_{n=0}^{\infty} \frac{(\alpha_1)_n}{(\alpha_2)_n} \frac{x^n}{n!}, \quad \alpha_2 \neq 0, -1, -2, \dots \quad (21)$$

where  $(\alpha)_n$  denoting the Pochhammer symbol defined in terms of the gamma function.

The temperature profile in terms of  $\eta$  is obtained as

$$\theta(\eta) = \left[ 1 + \frac{E_c P(1 + R_c S + \left( Mn + \frac{1}{K_p} \right) / r^2)}{(1 + R)(4 - (2S - Q)P_r^*)} \right] e^{-a\eta} \frac{M(a - 2, 1 + b, -P_r^* e^{-\eta})}{M(a - 2, 1 + b, -P_r^*)} \quad (22)$$

$$- \frac{E_c P(1 + R_c S + \left( Mn + \frac{1}{K_p} \right) / r^2)}{(1 + R)(4 - (2S - Q)P_r^*)} e^{-2r\eta}$$

The local Nusselt number is derived as

$$Nu_x Re_x^{-1/2} = -\theta'(0).$$

Case II: Power-law Heat Flux Case (PHF)

In case of PHF, introducing the similarity variable  $T - T_{\infty} = \frac{E_0 x^2}{K} \sqrt{\frac{\nu}{a}} \psi(\eta)$  and using equation (10), equation (8)

becomes

$$(1 + R)\psi'' + P_r f\psi' + P_r(Q - 2f')\psi = -E_c P_r(f''^2 + Rc(ff'' - ff''') + (Mn + 1/K_p)f'^2) \quad (23)$$

The boundary conditions are

$$\psi(0) = -1, \quad \psi(\infty) = 0 \quad (24)$$

The Eckert number for the PHF case is given by  $E_c = \frac{E^2 L^2 K \sqrt{E/\nu}}{BC_p}$  and the other parameters are as defined in the

PST case. Substituting  $\xi = -\frac{P_r e^{-\alpha\eta}}{(1 + R)r^2}$  into equations (23) and (24) yields

$$\begin{aligned} \xi \frac{d^2 \psi}{d\xi^2} + \left( 1 - \frac{P_r}{(1 + R)r^2} - \xi \right) \frac{d\psi}{d\xi} + \left( \frac{P_r Q}{(1 + R)r^2 \xi} + 2 \right) \psi \\ = -\frac{E_c (1 + R)r^2}{P_r} \left( 1 + R_c S + \frac{Mn + 1/K_p}{r^2} \right) \xi \end{aligned} \quad (25)$$

The boundary conditions are

$$\psi(\xi=0)=0, \psi'(\xi=-\frac{(1+R)r^2}{P_r})=-\frac{(1+R)r}{P_r} \quad (26)$$

The exact solution of (25) subject to the boundary conditions (26) can be written in terms of confluent hyper geometric function with similarity variable  $\eta$  and is given by

$$\psi(\eta) = \left[ \frac{1}{r} + 2 \frac{E_c P(1+R_c S + \left(Mn + \frac{1}{K_p}\right)/r^2)}{(1+R)(4-(2S-Q)P_r^*)} \right] e^{-a\eta} \frac{M(a-2, 1+b, -P_r^* e^{-\eta})}{aM(a-2, 1+b, -P_r^*) - P_r^* \frac{a-2}{b+1} M(a-1, 2+b, -P_r^*)} \quad (27)$$

$$- \frac{E_c P(1+R_c S + \left(Mn + \frac{1}{K_p}\right)/r^2)}{(1+R)(4-(2S-Q)P_r^*)} e^{-2\eta}$$

The local Nusselt number for PHF case can be expressed as

$$Nu_x Re_x^{-1/2} = 1/\psi(0).$$

## VI. NUMERICAL SOLUTION

The set of nonlinear coupled differential equations (11), (16) and (23) subject to the boundary conditions equations (12), (17) and (24) respectively constitute a two point boundary value problem. In order to solve these equations numerically we follow most efficient numerical shooting technique with sixth order Runge-Kutta scheme. In this method it is most important to choose the appropriate finite values of  $\eta \rightarrow \infty$ . To select  $\eta_\infty$  we begin with some initial guess value and solve the problem with some particular set of parameters to obtain  $f''(0)$ ,  $f'''(0)$ ,  $\theta'(0)$  and  $\psi'(0)$ . The solution process is repeated with another large values of  $\eta_\infty$  until two successive values of  $f''(0)$ ,  $f'''(0)$ ,  $\theta'(0)$  and  $\psi'(0)$  differ only after desired digit signifying the limit of the boundary along  $\eta$ . The last value of  $\eta_\infty$  is chosen as appropriate value of the limit  $\eta \rightarrow \infty$  for that particular set of parameters. The procedure is repeated until we get the results upto the desired degree of accuracy,  $10^{-6}$ .

## VII. RESULTS AND DISCUSSION

The present study considers the flow of a visco-elastic incompressible electrically conducting fluid flow past a stretching sheet through a porous medium in the presence of magnetic field, viscous dissipation, uniform heat source/sink, surface fluid suction/injection. The aim of the following discussion is to bring out the effect of permeability of the medium and plate temperature on the flow phenomena. The heat generation/absorption contributes significantly for non-isothermal heat transfer case. Another consideration of the present study is the saturated porous media. Porous media are very widely used to insulate a heated body to maintain its temperature. They are considered to be useful in diminishing the natural free convection which would otherwise occur intensely on the vertical surface.

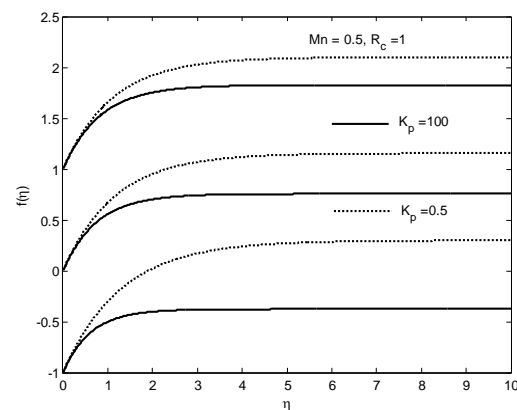


Fig. 1 (a) Transverse velocity profile with  $f_w = -1, 0, 1$

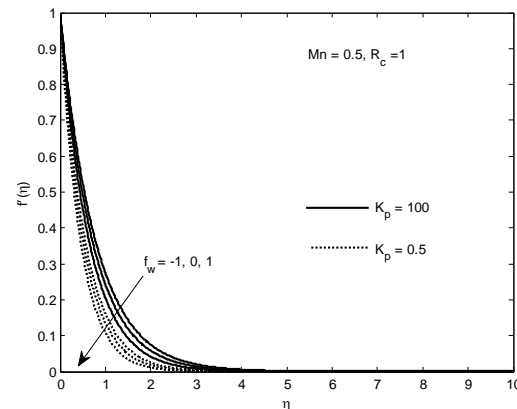


Fig. 1(b) Longitudinal velocity profile

Fig. 1(a) presents the effect of suction/injection parameter on transverse velocity profile for  $Mn = 0.5$  and for a second grade fluid  $R_c = 1$ . It is observed that the higher values of  $f_w$  enhance the velocity profile at all points in both the absence of  $K_p$  (i.e.  $K_p = 100$ ) and presence of  $K_p$  (i.e.  $K_p = 0.5$ ).

The effect of suction / injection on the longitudinal velocity profile in both the medium is illustrated in Fig. 1(b) for a second grade fluid with  $R_c = 1$ . In comparison to the impermeable sheet ( $f_w = 0$ ), it is

seen that suction ( $f_w > 0$ ) reduce the boundary layer thickness causes a decrease in velocity, where as injection ( $f_w < 0$ ) increases the velocity profile in both presence / absence of porous matrix.

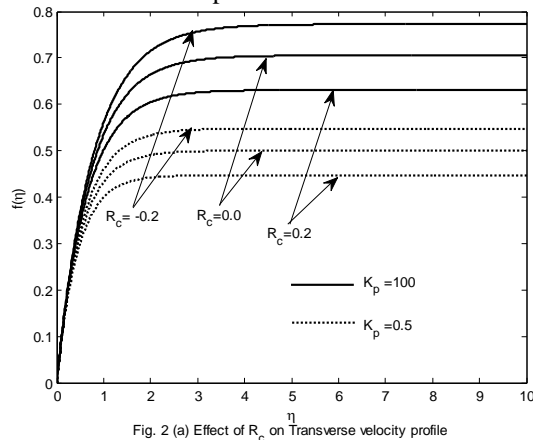


Fig. 2 (a) Effect of  $R_c$  on Transverse velocity profile

The effect of visco-elastic parameter  $R_c$  on the transverse velocity profile is shown in Fig. 2(a) for  $Mn=1, f_w=0$ . It is clear that  $R_c=0$ , the viscous fluid,  $R_c > 0$  stands for second-grade fluid and  $R_c < 0$  represents Walters liquid  $B'$ . In the absence of porous matrix  $K_p$  ( $K_p=100$ ), velocity of the fluid decreases with increase of visco-elastic parameter. The similar effect is noticed in the presence of  $K_p$  ( $K_p=0.5$ ). As compared to the viscous fluid ( $R_c=0$ ), the velocity decreases with increase in  $R_c$  (i.e. in case of second grade fluid,  $R_c > 0$ ) but the reverse trends follows with decrease in  $R_c$  (i.e. in case of Walters liquid  $B'$ ,  $R_c < 0$ ).

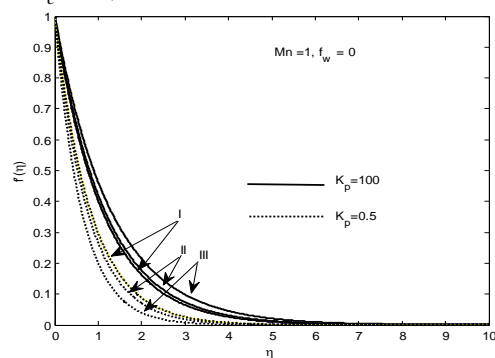


Fig.2(b) Longitudinal velocity profile with  $R_c = -0.2, 0, 0.2$

Fig.2(b) reveals the effect of visco-elastic parameter on longitudinal velocity profile for  $Mn=1, f_w=0$  in both absence/presence of porous matrix. In the absence of porous matrix, the velocity boundary layer thickness decreases with decrease in the value of  $R_c$ . It is

interesting to note that the reverse effect is observed in the presence of  $K_p$ .

Figs. 3(a) and 3(b) exhibit the variation of  $R_c$  on temperature profile in both PST and PHF case respectively, keeping

$P_r=3, Mn=1, E_c=0.1, R=1, S=0, f_w=0$  as fixed. It is observed that an increase in temperature due to the presence of elastic elements may be attributed to the fact that when an a visco-elastic fluid is in flow, a certain amount of energy is stored up in the material as strain energy in addition to viscous dissipation. In the absence of porous matrix  $K_p$  ( $K_p=100$ ), temperature of the fluid increases with increase of visco-elastic parameter. The similar effect is noticed in the presence of  $K_p$  ( $K_p=0.5$ ). In comparison to the viscous fluid

( $R_c=0$ ), the temperature increases as increase in  $R_c$  (i.e. in case of second grade fluid,  $R_c > 0$ ) but the reverse effect was found in decrease of  $R_c$  (i.e. in case of Walters liquid  $B'$ ,  $R_c < 0$ ). From fig.3(a) and 3(b), it is seen that the thermal boundary layer is asymptotic in nature.

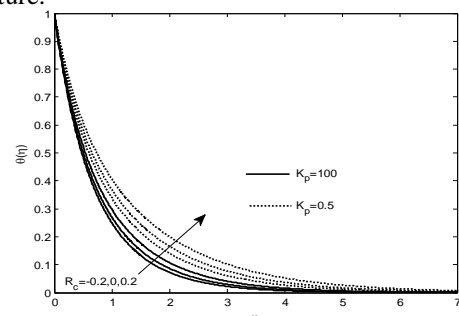


Fig.3(a) Temperature profile with  $P_r=3, Mn=1, E_c=0.1, R=1, Q=0, f_w=0$  (PST case)

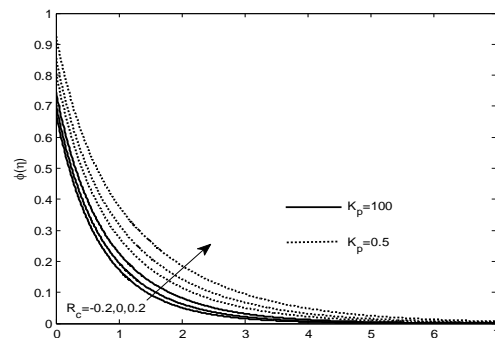


Fig.3(b) Temperature profile with  $P_r=3, Mn=1, E_c=0.1, R=1, Q=0, f_w=0$  (PHF case)

With the fixed values of  $P_r=3, Mn=1, R_c=1, R=1, S=0, f_w=0$ , effects of  $E_c$  on temperature profile in both PST and PHF case respectively are obtained from Fig. 4(a) and 4(b). An increase in  $E_c$  means more amount of heat energy is stored due to frictional heating leads to increase the temperature at all points in both PST and PHF case. In

the absence of  $K_p$  ( $K_p = 100$ , bold curves) and the presence of  $K_p$  ( $K_p = 0.5$ , dotted curves) temperature profile increases, in case of second grade fluid ( $R_c = 1$ ), as the value of the Eckert number increases.

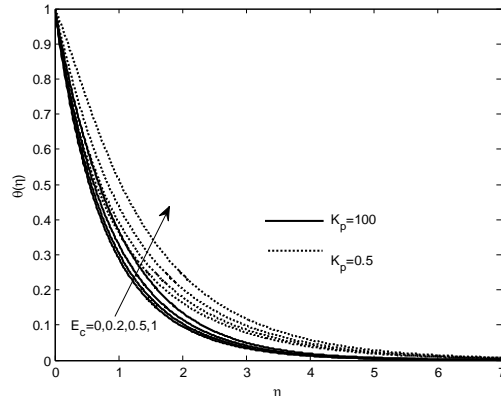


Fig.4(a) Temperature profile with  $P_r=1$ ,  $Mn=1$ ,  $R_c=1$ ,  $Q=0$ ,  $R=0$ ,  $f_w=0$  (PST case)

The dimensionless temperature profiles are presented for different values of Radiation parameter  $R$  for both PST and PHF cases with the fixed vales of other parameters e.g.,  $P_r = 3$ ,  $Mn = 1$ ,  $E_c = 0.1$ ,  $R_c = 0.5$ ,  $Q = 1$  in Fig. 5(a) and 5(b), respectively, in the absence/presence of porous matrix. A significant enhancement in the temperature profile is produced by increasing the thermal radiation parameter  $R$ . The thermal boundary layer thickness increases in both the presence/absence of  $K_p$  as well as wall temperature gradient decreases in PST case and surface temperature increases in PHF case. The results point out that thermal radiation is to reduce the heat transfer rate from the surface and thus, the radiation should be diminish to have the cooling process at a faster rate.

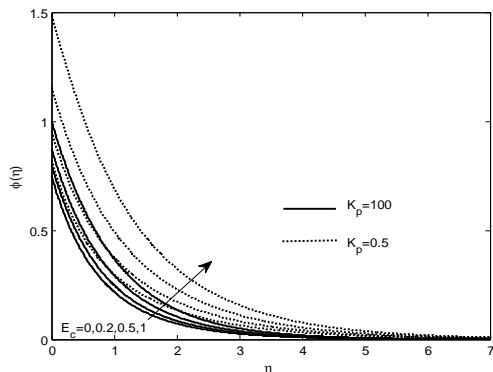


Fig 4(b) Temperature profile with  $P_r=3$ ,  $Mn=1$ ,  $E_c=0.1$ ,  $R_c=1$ ,  $Q=0$ ,  $f_w=0$  (PHF case)

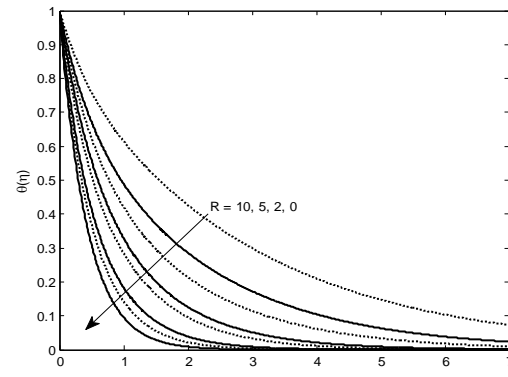


Fig. 5(a) Temperature profile with  $P_r = 3$ ,  $Mn=1$ ,  $E_c = 0.1$ ,  $R_c = 0.5$ ,  $Q = 0$ ,  $f_w = 0$  (PST case)

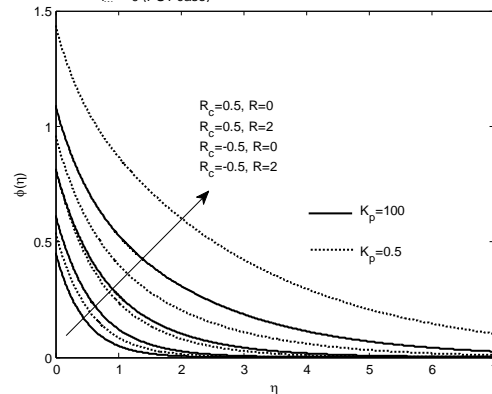


Fig. 5(b) Temperature profile with  $P_r=3$ ,  $Mn=1$ ,  $E_c=0.1$ ,  $Q=0$ ,  $f_w=0$  (PHF case)

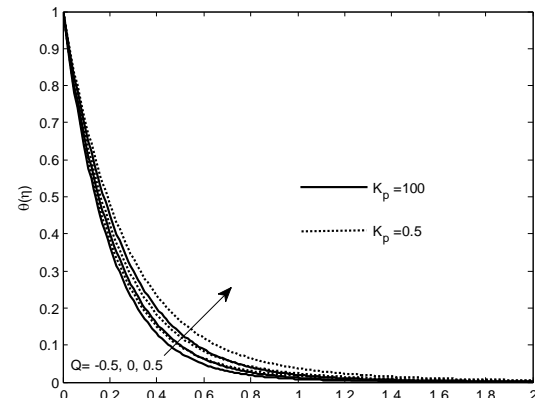


Fig. 6(a) Temperature profile with  $P_r=3$ ,  $Mn=1$ ,  $E_c=0.1$ ,  $R_c=0.5$ ,  $R=0$ ,  $f_w=0.5$  (PST case)

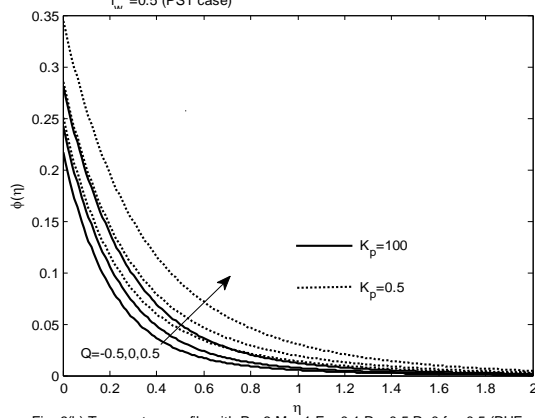


Fig. 6(b) Temperature profile with  $P_r=3$ ,  $Mn=1$ ,  $E_c=0.1$ ,  $R_c=0.5$ ,  $R=0$ ,  $f_w=0.5$  (PHF case)



In absence/presence of  $K_p$  the effect of internal heat generation/absorption parameter  $Q$  on the temperature distribution for PST and PHF cases with fixed values of the parameters  $P_r = 3, M_n = 1, E_c = 0.1, R_c = 0, f_w = 0.5$  is depicted through in Fig. 6(a) and 6(b). It is noticed that in case of heat source ( $Q > 0$ ), The energy generated in the thermal boundary layer causes the temperature profile to increase with the increasing value of  $Q$ , whereas in case of sink ( $Q < 0$ ) the temperature profile decreases with increasing the strength of heat absorption in both the absence of  $K_p$  ( $K_p = 100$ ) and presence of  $K_p$  ( $K_p = 0.5$ ).

Table-1: Skin friction coefficients for impermeable surface ( $f_w = 0$ )

Mn	Kp	Rc	$\tau$
1	100	-0.5	2.004993766
1	100	0	1.417744688
1	100	1	1.002496883
1	0.5	1	1.414213562
0.5	100	1	0.86890736
0.5	0.5	1	1.322875656
1	0.5	-0.5	2.828427125

From table 1 it is seen that an increasing magnetic parameter increases the skin friction and it is further increased by presences of porous matrix but the effect of elasticity is to decrease it. Thus, it is concluded presence of elastic elements each favourable in reducing the skin friction.

Table-2: Nusselt number For Walters liquid  $B'$  in absence of suction/blowing.

$P_r$	$R_c$	$Mn$	$K_p$	$Q$	$R$	PST case	PHF case
1	0	0	100	0	0	1.3333	0.750789
1	0	0	100	-0.1	0	1.3777965	0.7251
1	0	0	0.5	0	0	1.1268985	0.887391
1	0	0	0.5	-0.1	0	1.1993937	0.833755
1	0	1	100	0	0	1.2158	0.823201
1	0	1	100	-0.1	0	1.274028	0.7843
1	0	1	0.5	0	0	1.0553613	0.947543
1	0	1	0.5	-0.1	0	1.1403947	0.876889
1	-0.1	0.1	100	-0.1	0	1.3521	0.7395
1	-0.1	0.1	100	0	0	1.3035	0.7671
1	-0.1	0.1	100	0.1	0	1.2496	0.8002
1	-0.1	0.1	0.5	-0.1	0	1.1715398	0.853577
1	-0.1	0.1	0.5	0	0	1.0933434	0.914626
1	-0.1	0.1	0.5	0.1	0	0.9713764	1.026597
1	-0.1	0.1	100	-0.1	1	0.8812	1.1348
1	-0.1	0.1	0.5	-0.1	1	0.7223855	1.384303
2	-0.1	0.1	100	-0.1	0	2.021	0.4928
2	-0.1	0.1	0.5	-0.1	0	1.1715398	0.853577
3	-0.1	0.1	100	-0.1	0	2.5326	0.3926
3	-0.1	0.1	0.5	-0.1	0	2.3570593	0.424257

Table 2 and 3 reveal the comparison of temperature gradients for second grade and second order fluids in PST and PHF cases respectively. From table 2, it is observed that in the absence of porous matrix and magnetic parameter with higher Prandtl value Nusselt number increases irrespective of source/sink in PST case

whereas, the reverse effect is observed in PHF case. Further, it is seen that the presence of porous matrix attains the reverse trends in both PST and PHF cases. It is interesting to note that presence of magnetic parameter causes to decrease the Nusselt number in PST case and increase the same in PHF case in presence/absence of porous matrix and source/sink.

Thus, it is concluded that the characteristics of Nusselt number are obtained in the permeable surface ( $f_w = 0$ ) without thermal radiation ( $R = 0$ ) for second grade fluid. From table 3 it is observed that in the absence of porous matrix with high  $P_r$  Nusselt number increases in PST case and decreases in PHF case and the reverse effect is accomplished in the presence of the porous

matrix but increasing value of magnetic parameter, presence/absence of source/sink parameter and thermal radiation parameter cause the reverse effects in both PST and PHF cases. Therefore, the rate of heat transfer is sensitive to the presence of porous matrix, magnetic parameter and thermal radiation parameter causes instability in the rate of heat transfer phenomena.

Table-3: Nusselt Number For a second grade fluid with  $R_c = 1, E_c = 0.2, R = 0$  and  $f_w = 0$ .

$Mn$	$K_p$	$Q$	$P_r$	PST case	PHF case
0.0	100	-0.1	1	1.372608	0.7435
	100	-0.1	10	4.591724	0.277832
	0.5	-0.1	1	1.032946	0.975079
	0.5	-0.1	10	3.249158	0.536112
	100	0	1	1.331574	0.765383
	100	0	10	4.478859	0.28568
	0.5	0	1	0.974733	1.019901
	0.5	0	10	3.103711	0.55611
	100	0.1	1	1.288637	0.789645
	100	0.1	10	4.362827	0.294189
	0.5	0.1	1	0.906795	1.077075
	0.5	0.1	10	2.952014	0.578134
1.0	100	-0.1	1	1.181325	0.868455
	100	-0.1	10	3.87202	0.414209
	0.5	-0.1	1	0.906259	1.073528
	0.5	-0.1	10	2.676623	0.65084
	100	0	1	1.131589	0.901256
	100	0	10	3.741224	0.428464
	0.5	0	1	0.839487	1.132026
	0.5	0	10	2.518129	0.67632
	100	0.1	1	1.077335	0.939725
	100	0.1	10	3.605617	0.444078
	0.5	0.1	1	0.75274	1.216857
	0.5	0.1	10	2.352002	0.704501

### VIII. CONCLUSION

In this paper, the flow of a visco-elastic incompressible electrically conducting fluid flow past a stretching sheet through a porous medium in the presence of magnetic field, viscous dissipation, uniform heat source/sink, surface fluid suction/injection has been investigated. With the help of appropriate transformation, the governing boundary layer equations for momentum and thermal energy for both PHF and PST cases are reduced to coupled nonlinear ordinary differential equations which are then solved numerically using the shooting method and comparison has been made with that of confluent hypergeometric function. As a summary, we can conclude that

- Presence of porous matrix enhance the velocity because porous matrix act as insulator to the vertical surface preventing energy loss due to free convection.
- The resistive force of magnetic field is overcome due to the presence of porous matrix and elasticity of the fluid and hence the velocity increases due to the presence of both.
- Further, absence of magnetic field and porous matrix leads to transitory motion of the fluid.
- Presence of elasticity also leads to increase the temperature at all points but the presence of magnetic field reduce it.

- The thinning of thermal boundary layer thickness is due to slow rate thermal diffusion in presence of magnetic field and porous matrix.
- The variation in temperature is more sensitive due to presence of heat flux.
- Presence of elastic element is favorable in reducing the skin friction.
- The effect of porous matrix is duly compensated enhancing the magnetic strain in the absence of porous matrix on the rate of heat transfer.
- The rate of heat transfer in the present study is sensitive to the presence of porous matrix and magnetic parameter.

### REFERENCES

- [1] Paullet J., Weidman. Analysis of stagnation point flow forward a stretching sheet, *Int. J. Non-linear Mech.* 2008, 42, 1048-1091.
- [2] Crane L. J. Flow past a stretching plane, *Jape. Math. Phys. (ZAMP)* .1970, 21, 645-647.
- [3] Ishak A., Nazar R., Pop I. Unsteady mixed convection boundary layer flow due to a stretching vertical surface. *Arabian journal of Soci.Eng.* 2006, 31, 165-182.
- [4] Mahapatra T.R., Gupta A.S. Heat transfer in stagnation point flow towards a stretching sheet. *J. Heat Mass Transfer.* 2002, 38, 517-521.
- [5] Mahapatra T.R., Gupta A.S. Stagnation point flow towards a stretching surface. *Can. J. Chem. Eng.* 2003, 81, 258-263.
- [6] Sammer A.A. Heat and Mass Transfer Over an accelerating Surface with heat source in presence of magnetic field. *IJTAM.* 2009, 4, 281-293.
- [7] Wang C.Y. Stagnation flow towards a shrinking sheet. *Int. J. Non-linear Mecha.* 2008, 43, 377-382.
- [8] Naseem A., Khan N. Boundary layer flow past a stretching plate with suction and heat transfer with variable conductivity. *Int. J. Eng. And Material sciences.* 2000, 7, 51-53.
- [9] Elbashbeshy EMA., Bazid MAA. Heat transfer in a porous medium over a stretching surface with internal heat generation and suction or injection. *Appl. Math. Comp.* 2004,158, 799-807.
- [10] Cortell R. Flow and heat transfer of a fluid through a porous medium over a stretching surface with internal heat generation / absorption and suction/ blowing. *Fluid Dynamics Research.* 2005, 37, 231-245.
- [11] Anjali Devi S.P., Ganga B. Viscous dissipation effect on nonlinear MHD flow in a porous medium over a stretching porous surface. *Int. J. of Appl. Math. and Mech.* 2009, 5, 45-59.
- [12] Mushtaq M., Asghar S., Hossain M.A., Mixed convection flow of second grade fluid along a vertical stretching flat surface with variable surface temperature, *Heat and Mass Transfer,* 43(2007)1049-1061.
- [13] Hayat T., Abbas Z., Pop I., Mixed convection in the stagnation flow adjacent to a vertical surface in a visco-elastic fluid, *Int. J. Heat and Mass Transfer,* 51(2008) 3200-3206.
- [14] Arnold J.C., Asir A.A., Somasundarm S., Christopher T., Heat transfer in a visco-elastic boundary layer flow over a stretching sheet, *Int. J. Heat and Mass Transfer* 53(2010) 1112-1118.
- [15] Battaler R.C., Visco-elastic fluid flow and heat transfer over a stretching sheet under the effects of a non-uniform heat source, viscous dissipation and thermal radiation, *Int. J. Heat and Mass Transfer* 50(2007) 3152-3162.
- [16] Nadeem S., Mehmood R., Sher Akbar Noreen., Non-orthogonal stagnation point flow of a nano non-Newtonian fluid towards a stretching surface with heat transfer, *Int. J. Heat and Mass transfer,* 57(2013) 679-689.
- [17] Hayat T., Asad S., Qasim M. Hendi., Boundary layer flow of a Jeffery fluid with convective boundary conditions, *Int. J. Numer. Methods fluids,* 69(2012) 1350-1362.
- [18] Coleman B.D., Noll W., An approximation theorem for functional with applications in continuous mechanics, *Arch. Ration. Mech. Anal.,* 6(1960)355-370.
- [19] Rivlin R.S., Ericksen J.L., Stress deformation relations for isotropic materials, *J.Ration.Mech. Anal.*4(1955) 323-425.
- [20] Dunn J.E., Fosdick R.L., Thermodynamics, stability and boundedness of fluids of complexity 2 and fluids of second grade, *Arch. Ration.Mech. Anal.,* 56(1974) 191-252.
- [21] Beard D.W., Walters K., Elastico-viscous boundary layer flows: Part-I. Two dimensional flow near a stagnation point, *Proceedings in Cambridge Philos. Soc.,*(1964),667-674.
- [22] Chakrabarti A., Gupta A. S., Hydromagnetic flow and heat transfer over a stretching sheet, *Quart. Appl. Math.,* 37 (1979) 73-78.

